Optimized Irregular Variable Length Coding Design for Iteratively Decoded UltraWideBand Time-Hopping Spread-Spectrum Impulse Radio

R. A. Riaz[1,2], M. F. U. Butt[1,2], R. G. Maunder[1], S. X. Ng[1], S. Chen[1] and L. Hanzo[1]
[1]School of ECS, University of Southampton, SO17 1BJ, United Kingdom.
Email: {mfub06r, rar06r, sxn, lh}@ecs.soton.ac.uk, http://www-mobile.ecs.soton.ac.uk
[2]Dept of EE, COMSATS Institute of Information Technology, Islamabad, 44000, Pakistan, http://ciit.edu.pk

***Abstract*— Irregular Variable Length Coding Design for serial concatenated and iteratively decoded Time-Hopping (TH) Pulse Position Modulation (PPM) UltraWideBand (UWB) Spread-Spectrum (SS) Impulse radio system is considered. The proposed design is capable of low Signal-to-Noise Ratio (SNR) operation in Nakagami-m fading channel amalgamated with joint source and channel coding schemes. A number of component Variable Length Coding (VLC) codebooks with different coding rates are being utilized by IVLC scheme for encoding specific fractions of the input source symbol stream. The EXtrinsic Information Transfer (EXIT) charts are used to select these fractions in order to shape inverted EXIT curve of IVLC according to EXIT curve of the inner decoder match. The proposed scheme can achieve near-zero bit error ratio at low SNR values. This IVLC based scheme provides a gain of up to 0.45 dB over the identical-rate single class VLC based scheme.**

I. Introduction

The pioneering work in [1], [2] developed the concept of Time-Hopping (TH) Pulse Position Modulation (PPM) UWB impulse radio systems. In the aforesaid systems, trains of time shifted pulses through PPM are used to transmit base-band or carrierless UWB system information. Transmission performance is enhanced by the usage of multiple pulses to transmit a single symbol. One of the attractive features of TH-PPM-UWB systems is strong multipath interference mitigating capability.

Recently, UltraWideBand (UWB) systems have attracted substantial interest in the research community. UWB communications systems are commonly defined as systems that have either more than 20 percent relative bandwidth or more than 500 MHz absolute bandwidth. The large bandwidth of UWB leads to low sensitivity to fading, low interference to and from other systems along with accurate position location and ranging due to the fine time resolution [3], [4]. Heavy digital imaging and multimedia applications result in the requirements of high data rate wireless links. UWB has the capacity to fulfil the requirements of low cost and high speed digital indoor networks. 110 Mbps at a distance of 10m and 480 Mbps at a distance of 2m can be provided through UWB.

The financial support of COMSATS Institute of Information Technology, Islamabad under the auspices of Higher Education Commission, Pakistan and that of the EPSRC UK, as well as of the EU Optimix project is gratefully acknowledged.

Irregular Variable Length Coding (IVLC) uses a number of component Variable Length Coding (VLC) codebooks with different coding rates in order to encode specific fractions of the input source symbol stream [5]. The corresponding lengths of these fractions can be selected through EXtrinsic Information Transfer (EXIT) charts in order to shape the inverted EXIT curve of the IVLC so that it does not cross the EXIT curve of the inner channel [6]. This will enable to have an open EXIT chart tunnel at low values of Signal-to-Noise Ratio (SNR). The proposed design exploits this particular characteristic in an optimised manner.

In this contribution, we investigate for the first time an IVLC coding design for iteratively detected UWB TH Spread-Spectrum (SS) Impulse Radio in Nakagami-m fading channel. The EXIT charts technique is used to analyse the serial concatenation of Zero Forcing (ZF) detector, unity rate decoder and the IVLC outer decoder in order to achieve an improved performance at low SNR values.

The remaining paper is organised as follows. In Sec. II, the whole system design is elaborated. In Sec. III, TH-PPM-UWB transmission and detection is explained. In Sec. IV iterative decoding is discussed and the soft metrics are derived. In Sec. V, EXIT charts and Bit Error Ratio (BER) results are discussed for the choice of IVLC code parameters. Finally, in Sec. VI, we present our conclusions.

II. System Overview

The design considered in Fig. 1 assumes 16-ary source symbol values having probability density function (PDF) resulting from the Lloyd-Max (LM) quantization of independent Laplacian distribution. The variation bracket of the PDF lies between 0.002 and 0.16 with 4-bit LM quantization of a Gaussian source. The entropy communserating the PDF lies between 2.6 bits and 8.74 bits with an overall source entropy of 3.5 bits per VLC symbol.

The source symbol frame $\mathbf{\Psi}$ have 16-ary values with Q 4-bit source symbols $\{\Psi_q\}_{q=1}^{Q} \in [1 \dots 16]$. The source symbols constitutes Q components $\{\mathbf{\Psi^q}\}_{q=1}^{Q}$. The number of symbols in source symbol component Ψ^q obtained from source symbol frame Ψ is denoted by Q^q. In proposed design $Q^1 = Q$ is considered for benchmarker VLC based scheme and Q^{16}

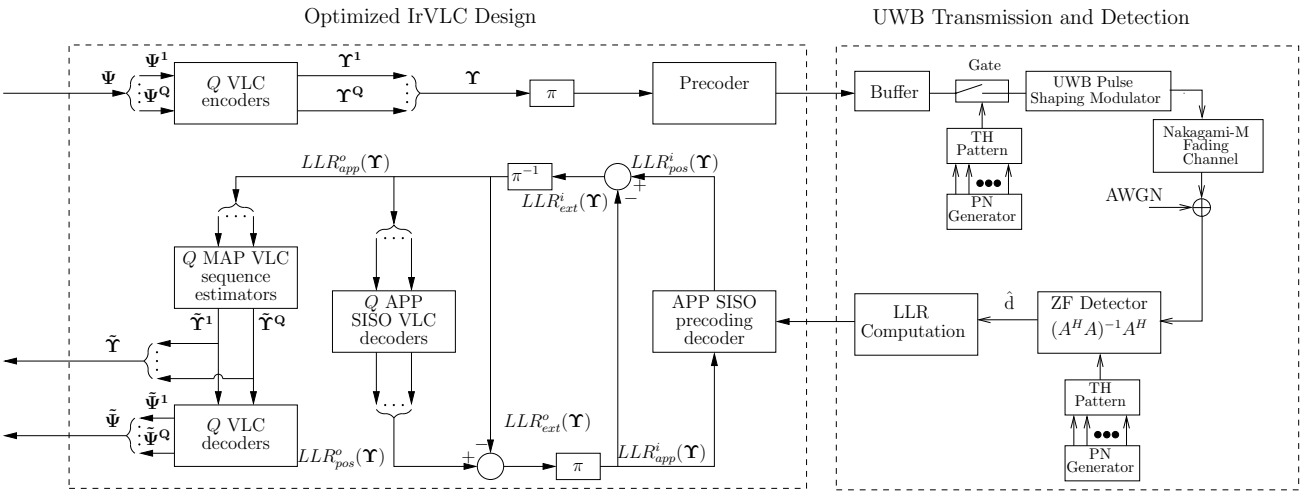

Fig. 1. Schematic of the IVLC and VLC-based TH-PPM-UWB schemes. In the IVLC coded scheme Q^{16}, whilst Q^1 in the VLC-coded scheme.

for IVLC-TH-PPM UWB. Furthermore IVLC-TH-PPM UWB scheme $\{Q^q\}_{q=1}^{Q}$ values are selected so inverted EXIT curve of the IVLC does not cross the EXIT curve of inner encoder.

The transmission frame component $\boldsymbol{\Upsilon^{\mathbf{q}}} = \{\mathbf{VLC}^{q,\Psi_{jq}^{q}}\}_{q^q=1}^{Q^q}$ is the concatenation of Q^q number of VLC codewords that represent the Q^q number of source symbols in the source symbol frame component $\boldsymbol{\Psi^{\mathbf{q}}}$. The codeword $\mathbf{VLC}^{q,k}$ having length $W^{q,k}$ represents specific source symbols having the value of $k \in [1 \dots 16]$ encoded by the corresponding VLC code book $\mathbf{VLC}^q$.The VLC-encoder corresponding to codebook form the set of Q number of VLC codebooks $\{\mathbf{VLC}^q\}_{q=1}^{Q}$ have range of coding rates $\{R^q\}_{q=1}^{Q} \in [0, 1]$.

The concatenated frame $\boldsymbol{\Psi}$ from components $\{\boldsymbol{\Psi^{\mathbf{q}}}\}_{q=1}^{Q}$ as shown in Fig. 1 has a length of $\sum_{q=1}^{Q} W^q$ bits. The interleaved and precoded bits are sent to buffer as depicted by the schematic 1. These bits are transmitted by the TH-PPM modulator. In TH-PPM-UWB the transmitted TH-UWB signal conveying the M-ary symbol is generated by invoking several frames. Let one symbol invokes L number of frames. The frame time T_F is related to the symbol interval T_S by $T_S = LT_F$. Furthermore with in a frame the desired time shift T_{CH} is generated by TH code. As depicted in Fig. 1 we have used pseudo-noise (PN) generator for this purpose. The details of UWB Transmission will be discussed in the next section.

In this paper, TH-PPM-UWB evaluated using UWB multipath channel model based on indoor channel measurements between 3.1 GHZ to 10.6 GHz over a range of less than 10 meters. The UWB channels follow lognormal or Nakagami distribution. The transmitted signal is also corrupted by Additive White Gaussian Noise (AWGN) and a Jamming signal having single-sided power spectral densities of N_0 and N_J, respectively.

The receiver schematic is also shown in Fig. 1, where the Zero Forcing Detector is used to estimate the data $\hat{\mathrm{d}}$. The ZFD has the capability to combat Multiple Access Interference (MAI) and Inter-Symbol Interference (ISI) at the expense of enhancing noise at low SNR. After the ZFD, the corresponding symbol probabilities and log-likelihood ratios (LLRs) are computed, as explained in the section IV, which are then fed to the unity-rate decoder of Fig. 1.

III. UWB Transmission and Detection

A. TH PPM UWB

A general TH-PPM-UWB signal is given by [7]

$$g(t) = \sum_{n=-\infty}^{\infty} \phi(t - nT_F - T_{PP_n} - T_{CH_n}), \qquad (1)$$

where $\phi(t)$ is reference pulse shape, T_F is the frame time, T_{PP_n} is small shift in the pulse position, either forward or backward to represent the binary stream, T_{CH_n} is the time shift based on time hopping code where the code repeats after a certain interval. The pulse repetition frequency (PRF) is reciprocal of T_F. The frame time T_F will be of the order of 1000 times the actual pulse width to avoid interference from reflected pulses.

As shown in Fig. 1, for Time Hopping pattern we have used Pseudo-Noise (PN) codes. PN Codes have the Auto-CorreLation (ACL) and Cross-CorreLation (CCL) properties, which are best for combating Inter-Symbol Interference (ISI) and Multi-Access Interference (MAI).

B. Channel Model

In this contribution, TH-PPM-UWB is evaluated using UWB multipath channel model based on indoor channel measurements between 3.1 GHZ to 10.6 GHz over a range of less than 10 meters. The model accepted by IEEE 802.15.3 and considered can be expressed as [8]

$$h(t) = \sum_{r=1}^{R} h_r e^{j\varphi_r} \delta(t - rT_\varphi) \qquad (2)$$

where R represents the number of resolvable multipaths, h_r and φ_r are the gain and phase of the rth resolvable multipath

component. While rT_φ represent the corresponding delay of the rth multipath component.

As shown in [9], [10] the measured data shows that the UWB channels follow lognormal or Nakagami distribution, which has been validated by using the Kolmogorov-Smirnov testing with a significance level of 1 percent. The fading gain amplitude h_r comply the independent Nakagami-m distribution for our analysis with a probability density function (PDF) of the envelop c is given by [11]

$$P_{h_r}(c) = \frac{2m_r^{m_r} r^{2m_r-1}}{\Gamma(m_r)\Omega_r^{m_r}} e^{\frac{-m_r c^2}{\Omega_r}}, \qquad c > 0 \tag{3}$$

where m_r is the fading parameter defined as:

$$m_r = \frac{E^2\left[c^2\right]}{var(c^2)} \tag{4}$$

The parameter Ω_r is

$$\Omega_r = E\left[c^2\right] \tag{5}$$

Further the moments of random variable c is given by:

$$E\left[c^v\right] = \frac{\Gamma\left(m_r + \frac{v}{2}\right)}{\Gamma(m_r)} \left(\frac{\Omega}{m_r}\right)^{\frac{v}{2}} \tag{6}$$

Finally $\Gamma(\cdot)$ is the gamma function defined as

$$\Gamma(m_r) = \int_0^\infty x^{m_r-1} e^{(-x)} dx \tag{7}$$

We assume in our analysis that the phase rotation due to fading channel is uniformly distributed in $[0, 2\pi]$. Let us now consider the receiver structure.

The transmitted signal is also corrupted by Additive White Gaussian Noise (AWGN) and a Partial Band Noise Jamming (PBNJ) signal having single-sided power spectral densities of N_0 and N_J, respectively. We assume that the PBNJ signal jams a fraction $0 \leq \rho \leq 1$ of the total spread spectrum bandwidth W_{ss}. We also assume that the PBNJ signal is contiguous. Thus, the probability that a band or a tone is jammed is given by ρ, while the probability that the band is not jammed is $(1-\rho)$.

C. Receiver Model

Zero Forcing Detector The discretized received composite signal can be represented in matrix form as [12]:

$$\mathbf{y} = \mathbf{Ad} + \mathbf{n}, \tag{8}$$

where $\mathbf{n}$ is the noise sequence, which has a covariance matrix of $\mathbf{R}_n = E[nn^H]$, $\mathbf{A}$ is overall system matrix and $\mathbf{d}$ is user data vector. The data estimates at the output of Zero Forcing Detector (ZFD) is

$$\hat{\mathbf{d}}_{\mathbf{ZFD}} = \underbrace{\mathbf{d}}_{Data} + \underbrace{(\mathbf{A^H R_n^{-1} A})^{-1} \mathbf{A^H R_n^{-1} n}}_{Noise}, \tag{9}$$

If it is assumed that in Eq (9) $\mathbf{n}$ consists of noise samples that are zero mean Gaussian variables having a variance of σ^2, then its covariance matrix is $\mathbf{R}_n = \sigma^2 I$ where I is the identity matrix, Eq (9) can be reduced to

$$\hat{\mathbf{d}}_{\mathbf{ZFD}}\Big|_{\mathbf{R}_n=\sigma^2 I} = (\mathbf{A^H A})^{-1} \mathbf{A^H y}, \tag{10}$$

It is evident from Eqs (9) and (10) that ZFD decorrelates the MAI and ISI and forces them to zero. However the removal of ISI and MAI is performed at the expense of noise enhancement.

IV. Iterative decoding

The Conditional Probability for the jth transmitted symbol Ψ_j where $j = 0, \ldots, J-1$ given that the signal $\hat{\mathbf{d}} = \left[d_0, d_1, \ldots, d_{J-1}\right]$ which represent the set of J outputs of the ZFD Detector Fig. 1 is given by

$$P(\Psi_j|\hat{\mathbf{d}}) = \frac{p(\hat{\mathbf{d}}|\Psi_j)P(\Psi_j)}{p(\hat{\mathbf{d}})}, \tag{11}$$

where $p(\hat{\mathbf{d}}|\Psi_j)$ is the Probability Density Function (PDF) of the received signal $\hat{\mathbf{d}}$, given that Ψ_j is transmitted. Furthermore, $P(\Psi_j)$ is the *a priori* probability of the symbol Ψ_j, while $p(\hat{\mathbf{d}}) = \sum_{j=0}^{J-1} p(\hat{\mathbf{d}}|\Psi_j)P(\Psi_j)$ is the probability of receiving signal set $\hat{\mathbf{d}}$. For transmitted symbols $P(\Psi_j) = 1/J$, PDF $p(\hat{\mathbf{d}}|\Psi_j)$ uniquely determine the statistics for estimating the probability $P(\Psi_j|\hat{\mathbf{d}})$. The expression for $p(\hat{\mathbf{d}}|\Psi_j)$ is given by

$$p(\hat{\mathbf{d}}|\Psi_j) = f_{d_j}(v_j|\Psi_j) \prod_{x=0, x\neq j}^{J-1} f_{d_n}(v_x|\Psi_j), \tag{12}$$

where $f_{d_n}(v_x|\Psi_j)$ represents the PDF of the xth detector value, $x = 0, 1, \ldots, J-1$, given that Ψ_j is transmitted. The simplified expression for $p(\hat{\mathbf{d}}|\Psi_j)$ is

$$p(\hat{\mathbf{d}}|\Psi_j) = \exp\left(\frac{v_j \gamma_h}{1+\gamma_h}\right), \tag{13}$$

where $\gamma_h = bRE_b/(N_0 L)$ is the SNR per hop, R is the code rate, E_b is the transmitted energy per bit and $b = \log_2 M$ is the number of bits per symbol. From Eqs. (12) and (13) corresponding LLRs can be computed [13].

The Mutual Information are based on histogram method approximation of the true distribution. In Fig. 1 LLR_y^x denotes the Log Likelihood Ratios, where x refers to inner or outer encoder and decoders, y is for *a priori, a posteriori* or extrinsic information respectively. In perspective of more convincing concatenation, outer EXIT curve of a half-rate Recursive Systematic Convolutional (RSC) decoder characterised by the octal generator polynomial of (7,5) and inner decoder EXIT curve of a precoder by the generator polynomial of $1/(1+D)$ is being used for the design.

The *a posteriori probabilities* (app) SISO unity rate decoder and the outer decoder perform iterative decoding, as shown in Fig. 1, both invoking the Bahl-Cocke-Jelinek-Raviv (BCJR) algorithm [14] on the basis of bit-based trellises [15]. Extrinsic soft information, in the form of LLRs, is iteratively exchanged between the rate-1 decoder and the VLC decoding stages for

the sake of assisting each other's operation in the usual fashion, as detailed in [16]. Since Q number of separate VLC encoders and decoders are used in transceivers Fig. 1. Each of the Q number of VLC decoders is provided with the *a priori* LLR sub-frame $LLR^o_{app}(\mathbf{\Psi^q})$ and in response it generates the *a posteriori* LLR sub-frame $LLR^o_{pos}(\mathbf{\Psi^q})$, $q \in [1 \dots Q]$. These *a posteriori* LLR sub-frames are concatenated in order to provide the *a posteriori* LLR frame $LLR^o_{pos}(\mathbf{\Psi})$, as shown in Fig. 1.

Each transmission frame component $\mathbf{\Psi^q}$ is estimated from the corresponding *a priori* LLR frame component $LLR^o_{app}(\mathbf{\Psi^q})$ in final iteration. The transmission frame component estimates $\tilde{\mathbf{\Psi}}^{\mathbf{q}}$ may be VLC decoded to provide the source symbol frame component estimates $\tilde{\mathbf{\Upsilon}}^{\mathbf{q}}$ after concatenating transmission frame components. Finally these symbol frame component estimates $\tilde{\mathbf{\Upsilon}}^{\mathbf{q}}$ are concatenated to generate the source symbol frame estimates $\tilde{\mathbf{\Upsilon}}$ as shown in Fig. 1.

In the next section we detail the design of our IVLC TH-PPM-UWB scheme with the aid of EXIT chart analysis.

V. System parameters and Simulation Results

In our proposed design of IVLC-TH-PPM-UWB scheme, VLC codebooks $\{\mathbf{VLC}^q\}_{q=1}^{Q}$ with component size 16 having approximately coding rates in range $[0.25, 0.95]$ are used. Furthermore Variable Length Error Correcting (VLEC) codebook is utilised. For VLC scheme VLC codebook with one component, analogous to IVLC-TH-PPM-UWB scheme$\mathbf{VLC}^{10}$ with coding Rate $R = 0.5$ is employed

Fig. 2. depicts the inverted EXIT curves for the bit based app SISO VLC decoding of the aforsaid VLC codebooks combined with unity rate decoder's EXIT curves at E_b/N_0 values of 6.4 and 6.5 dB in Nakagami-m fading channel. Having equiprobable transmission frame's bits EXIT curves are generated using uncorrelated Gaussian distributed *a priori* LLRs. The inverted EXIT curve of the IVLC scheme shown in Fig. 2 was generated by appropriately weighted superposition of the 16 component VLC codebooks inverted EXIT curves. The specific number of source symbols employed to encode Q^q is proportional to the weight applied to the inverted EXIT curve of the component VLC codebook $\mathbf{VLC^q}$.

Using algorithm of [17] it has been found that only 4 of the 16 VLC components can be used to encode a non-zero number of source symbols in order to make sure that IVLC coding rate matches that of regular VLC scheme namely 0.5. Furthermore these 4 components also ensure that the inverted IVLC EXIT curve did not cross the unity rate decoder EXIT curve at E_b/N_0 of 6.4 dB. It can easily be seen from Fig. 2 that an infinitesimally low BER can be achieved by the IVLC-TH-PPM-UWB scheme for E_b/N_0 values above 6.4dB by the presence of the resultant open EXIT chart tunnel. This is not possible for the peer VLC based scheme for E_b/N_0 values below 6.5 dB. The values of VLC codebooks along with rates are mentioned in the Table. I used for Fig. 2.

Analogous to the IVLC design of Fig. 2 created for the interference-free channel, we have also designed an IVLC code for the Nakagami-m fading channel with interference, assuming $E_b/N_J = 10$dB and interference fraction of $\rho = 0.1$. The values of $J^n, n = 1, \dots, 16$ optimized for this particular jammed channel are $[0\ 0\ 0\ 0.22\ 0\ 0\ 0\ 0.27\ 0\ 0.05\ 0\ 0.3\ 0\ 0\ 0\ 0]$.

Fig. 3 corroborates the results of Fig. 2 by recording the

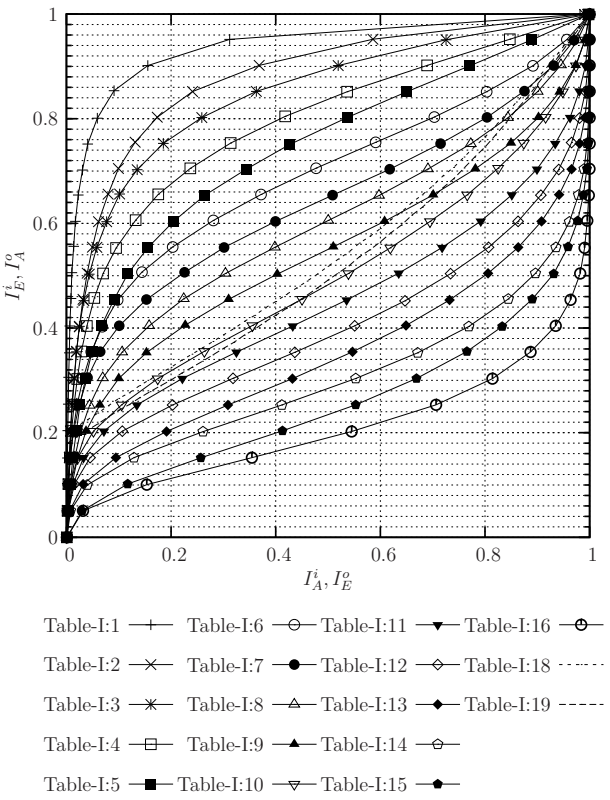

Fig. 2. Inverted VLC EXIT curves and unity rate decoder EXIT curves, assuming an interference-free, uncorrelated Nakagami-m fading channel.

TABLE I
VLC Parameters and Code Rates

1. VLC^1, R^1=0.95, Q^1=0	11. VLC^{11}, R^{11}=0.45, Q^{11}=0
2. VLC^2, R^2=0.89, Q^2=0	12. VLC^{12}, R^{12}=0.4, Q^{12}=0.5Q
3. VLC^3, R^3=0.85, Q^3=0	13. VLC^{13}, R^{13}=0.35, Q^{13}=0
4. VLC^4, R^4=0.8, Q^4=0.18Q	14. VLC^{14}, R^{14}=0.3, Q^{14}=0
5. VLC^5, R^5=0.75, Q^5=0	15. VLC^{15}, R^{15}=0.25, Q^{15}=0
6. VLC^6, R^6=0.7, Q^6=0.12Q	16. VLC^{16}, R^{16}=0.2, Q^{16}=0
7. VLC^7, R^7=0.65, Q^7=0	17. $IVLC$=0.5
8. VLC^8, R^8=0.60, Q^8=0.2Q	18. $PrecoderSNR$=6.5dB
9. VLC^9, R^9=0.55, Q^9=0	19. $PrecodeSNR$=6.4dB
10. VLC^{10}, R^{10}=0.5, Q^{10}=0.2Q	20. EXIT Open Tunnel 6.4dB

MI values at the output of the inner and outer decoders. The trajectory steps follows the EXIT curves of the inner and outer IVLC decoder. Furthermore the BER versus E_b/N_0 results of Fig. 4 verifies the performance predictions of Fig. 3. The assumptions for both Fig. 3 and 4 are $E_b/N_J = 10$dB, source symbol values 16 and precoder memory $L = 3$. The improvement in BER can be achieved at an expense of increase complexity and number of decoding iterations without precoder.

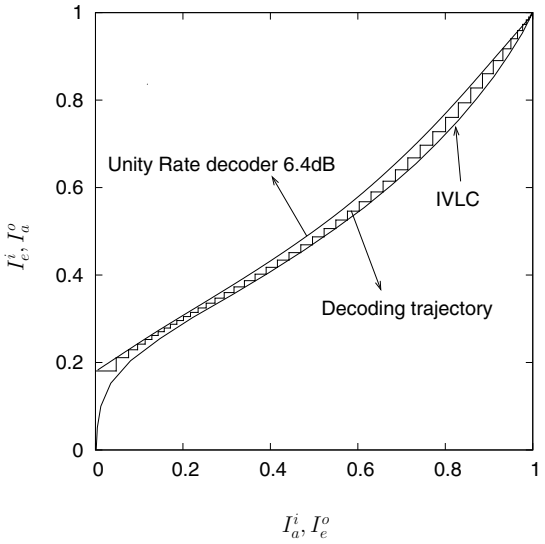

Fig. 3. IVLC and unity rate decoder EXIT curves as well as decoding trajectory, assuming an interference-free, uncorrelated Nakagami-m fading channel.

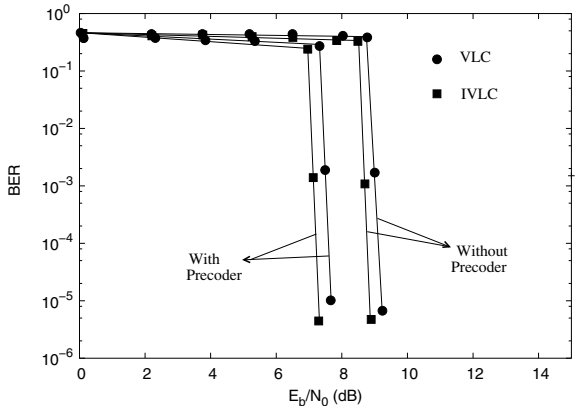

Fig. 4. BER versus SNR performance of the VLC and IVLC based schemes, in jammed as well as an interference-free, uncorrelated Nakagami-m fading channels with 30 iterations.

VI. Conclusion

We have investigated the serial concatenation design of IVLC coding with a TH-PPM-UWB operating in a Nakagami-m fading channel. The unity rate code make the channel recursive and IVLC code was design in such a way that an open EXIT chart tunnel is created even at low SNR values. Furthermore, the inverted EXIT curve of the IVLC decoder matches the EXIT curve of the inner decoder.

The purposed IVLC TH-PPM-UWB design provides additional performance gain of up to 0.45dB over VLC-based scheme. In our future work, we will investigate more sophisticated three-stage iterative decoding, through exchange of extrinsic information amongst the detector, the unity rate decoder and the outer decoder.

References

[1] M. Z. Win and R. A. Scholtz, "Impulse radio: how it works," *IEEE Communications Letters*, vol. 2, pp. 36–38, Feb. 1998.

[2] M. Z. Win and R. A. Scholtz, "Ultra-wide bandwidth time-hopping spread-spectrum impulse radio forwireless multiple-access communications," *IEEE Transactions on Communications*, vol. 48, pp. 679–689, Apr. 2000.

[3] S. Gezici, Z. Tian, G. B. Giannakis, H. Kobayashi, A. F. Molisch, H. V. Poor, and Z. Sahinoglu, "Localization via ultra-wideband radios: a look at positioning aspects for future sensor networks," *IEEE Signal Processing Magazine*, vol. 22, pp. 70–84, July 2005.

[4] M. Z. Win and R. A. Scholtz, "On the energy capture of ultrawide bandwidth signals in densemultipath environments," *IEEE Communications Letters*, vol. 2, pp. 245–247, Sept. 1998.

[5] V. Buttigieg and P. G. Farrell, "Variable-length error-correcting codes," *IEE Proceedings on Communications*, vol. 147, pp. 211–215, August 2000.

[6] R. G. Maunder, J. Wang, S. X. Ng, L.-L. Yang, and L. Hanzo, "Iteratively Decoded Irregular Variable Length Coding and Trellis Coded Modulation," in *IEEE Workshop on Signal Processing Systems*, (Shanghai, China), October 2007.

[7] R. A. Riaz, M. El-Hajjar, Q. Z. Ahmed, S. X. Ng, S. Chen, and L. Hanzo, "Convergence Analysis of Iteratively Detected Time Hopping and DS-CDMA Ultrawide Bandwidth Systems by EXIT Charts," in *Proceedings of the IEEE Vehicular Technology Conference, 2008.*, pp. 1127 – 1131, May 2008.

[8] H. Sato and T. Ohtsuki, "Frequency domain channel estimation and equalisation for direct sequence ultra wideband (DS-UWB) system," *IEE Proceedings- Communications*, vol. 153, pp. 93–98, Feb. 2006.

[9] A. F. Molisch, "Ultrawideband propagation channels-theory, measurement, and modeling," *IEEE Transactions on Vehicular Technology*, vol. 54, pp. 1528–1545, Sept. 2005.

[10] R. A. Riaz, M. F. U. Butt, S. Chen, and L. Hanzo, "Generic z-domain discrete-time transfer function estimation for ultra-wideband systems," *Electronics Letters*, vol. 44, pp. 1491–1492, Dec. 2008.

[11] M. D. Yacoub, J. E. V. Bautistu, and L. Guerra de Rezende Guedes, "On higher order statistics of the nakagami-m distribution," *IEEE Transactions on Vehicular Technology*, vol. 48, pp. 790–794, May 1999.

[12] L. Hanzo, L.-L. Yang, E.-L. Kuan, and K. Yen, *Single- and Multi-Carrier DS-CDMA: Multi-User Detection, Space-Time Spreading, Synchronisation, Networking and Standards*. New York: John Wiley and Sons, England, 2003.

[13] S. ten Brink, "Convergence of iterative decoding," *IEEE Transactions on Communications*, vol. 49, pp. 1727 – 1737, October 2001.

[14] L. Bahl, J. Cocke, F. Jelinek, and J. Raviv, "Optimal decoding of linear codes for minimizing symbol error rate (Corresp.)," *IEEE Transactions on Information Theory*, vol. 20, no. 2, pp. 284–287, 1974.

[15] V. B. Balakirsky, "Joint source-channel coding with variable length codes," in *IEEE International Symposium on Information Theory*, (Ulm, Germany), June 1997.

[16] S. Benedetto and G. Montorsi, "Serial concatenation of block and convolutional codes," *Electronics Letters*, vol. 32, no. 10, pp. 887–888, 1996.

[17] M. Tüchler and J. Hagenauer, "EXIT charts of irregular codes," in *Conference on Information Sciences and Systems*, (Princeton, NJ), pp. 748–753, March 2002.